

Probing neutrino emission at GeV energies from compact binary mergers with the IceCube Neutrino Observatory

R. Abbasi,¹⁷ M. Ackermann,⁵⁹ J. Adams,¹⁸ J. A. Aguilar,¹² M. Ahlers,²² M. Ahrens,⁵⁰ C. Alispach,²⁸ A. A. Alves Jr.,³¹ N. M. Amin,⁴² R. An,¹⁴ K. Andeen,⁴⁰ T. Anderson,⁵⁶ I. Anseau,¹² G. Anton,²⁶ C. Argüelles,¹⁴ Y. Ashida,³⁸ S. Axani,¹⁵ X. Bai,⁴⁶ A. Balagopal V.,³⁸ A. Barbano,²⁸ S. W. Barwick,³⁰ B. Bastian,⁵⁹ V. Basu,³⁸ S. Baur,¹² R. Bay,⁸ J. J. Beatty,^{20,21} K.-H. Becker,⁵⁸ J. Becker Tjus,¹¹ C. Bellenghi,²⁷ S. BenZvi,⁴⁸ D. Berley,¹⁹ E. Bernardini,^{59,*} D. Z. Besson,^{33,†} G. Binder,^{8,9} D. Bindig,⁵⁸ E. Blaufuss,¹⁹ S. Blot,⁵⁹ F. Bontempo,³¹ J. Borowka,¹ S. Böser,³⁹ O. Botner,⁵⁷ J. Böttcher,¹ E. Bourbeau,²² F. Bradascio,⁵⁹ J. Braun,³⁸ S. Bron,²⁸ J. Brostean-Kaiser,⁵⁹ S. Browne,³² A. Burgman,⁵⁷ R. S. Busse,⁴¹ M. A. Campana,⁴⁵ C. Chen,⁶ D. Chirkin,³⁸ K. Choi,⁵² B. A. Clark,²⁴ K. Clark,³⁴ L. Classen,⁴¹ A. Coleman,⁴² G. H. Collin,¹⁵ J. M. Conrad,¹⁵ P. Coppin,¹³ P. Correa,¹³ D. F. Cowen,^{55,56} R. Cross,⁴⁸ P. Dave,⁶ C. De Clercq,¹³ J. J. DeLaunay,⁵⁶ H. Dembinski,⁴² K. Deoskar,⁵⁰ S. De Ridder,²⁹ A. Desai,³⁸ P. Desiati,³⁸ K. D. de Vries,¹³ G. de Wasseige,^{13,‡} M. de With,¹⁰ T. DeYoung,²⁴ S. Dharani,¹ A. Diaz,¹⁵ J. C. Díaz-Vélez,³⁸ H. Dujmovic,³¹ M. Dunkman,⁵⁶ M. A. DuVernois,³⁸ E. Dvorak,⁴⁶ T. Ehrhardt,³⁹ P. Eller,²⁷ R. Engel,^{31,32} H. Erpenbeck,¹ J. Evans,¹⁹ P. A. Evenson,⁴² A. R. Fazely,⁷ S. Fiedlschuster,²⁶ A.T. Fienberg,⁵⁶ K. Filimonov,⁸ C. Finley,⁵⁰ L. Fischer,⁵⁹ D. Fox,⁵⁵ A. Franckowiak,^{11,59} E. Friedman,¹⁹ A. Fritz,³⁹ P. Fürst,¹ T. K. Gaisser,⁴² J. Gallagher,³⁷ E. Ganster,¹ A. Garcia,¹⁴ S. Garrappa,⁵⁹ L. Gerhardt,⁹ A. Ghadimi,⁵⁴ C. Glaser,⁵⁷ T. Glauch,²⁷ T. Glüsenkamp,²⁶ A. Goldschmidt,⁹ J. G. Gonzalez,⁴² S. Goswami,⁵⁴ D. Grant,²⁴ T. Grégoire,⁵⁶ S. Griswold,⁴⁸ M. Gündüz,¹¹ C. Günther,¹ C. Haack,²⁷ A. Hallgren,⁵⁷ R. Halliday,²⁴ L. Halve,¹ F. Halzen,³⁸ M. Ha Minh,²⁷ K. Hanson,³⁸ J. Hardin,³⁸ A. A. Harnisch,²⁴ A. Haungs,³¹ S. Hauser,¹ D. Hebecker,¹⁰ K. Helbing,⁵⁸ F. Henningsen,²⁷ E. C. Hettinger,²⁴ S. Hickford,⁵⁸ J. Hignight,²⁵ C. Hill,¹⁶ G. C. Hill,² K. D. Hoffman,¹⁹ R. Hoffmann,⁵⁸ T. Hoinka,²³ B. Hokanson-Fasig,³⁸ K. Hoshina,^{38,§} F. Huang,⁵⁶ M. Huber,²⁷ T. Huber,³¹ K. Hultqvist,⁵⁰ M. Hünnefeld,²³ R. Hussain,³⁸ S. In,⁵² N. Iovine,¹² A. Ishihara,¹⁶ M. Jansson,⁵⁰ G. S. Japaridze,⁵ M. Jeong,⁵² B. J. P. Jones,⁴ R. Joppe,¹ D. Kang,³¹ W. Kang,⁵² X. Kang,⁴⁵ A. Kappes,⁴¹ D. Kappesser,³⁹ T. Karg,⁵⁹ M. Karl,²⁷ A. Karle,³⁸ U. Katz,²⁶ M. Kauer,³⁸ M. Kellermann,¹ J. L. Kelley,³⁸ A. Kheirandish,⁵⁶ K. Kin,¹⁶ T. Kintscher,⁵⁹ J. Kiryluk,⁵¹ S. R. Klein,^{8,9} R. Koirala,⁴² H.

Kolanoski,¹⁰ T. Kontrimas,²⁷ L. Köpke,³⁹ C. Kopper,²⁴ S. Kopper,⁵⁴ D. J. Koskinen,²² P. Koundal,³¹ M. Kovacevich,⁴⁵ M. Kowalski,^{10,59} N. Kurahashi,⁴⁵ A. Kyriacou,² N. Lad,⁵⁹ C. Lagunas Gualda,⁵⁹ J. L. Lanfranchi,⁵⁶ M. J. Larson,¹⁹ F. Lauber,⁵⁸ J. P. Lazar,^{14,38} J. W. Lee,⁵² K. Leonard,³⁸ A. Leszczyńska,³² Y. Li,⁵⁶ Q. R. Liu,³⁸ M. Liubarska,²⁵ E. Lohfink,³⁹ C. J. Lozano Mariscal,⁴¹ L. Lu,³⁸ F. Lucarelli,²⁸ A. Ludwig,^{24,35} W. Luszczyk,³⁸ Y. Lyu,^{8,9} W. Y. Ma,⁵⁹ J. Madsen,³⁸ K. B. M. Mahn,²⁴ Y. Makino,³⁸ S. Mancina,³⁸ I. C. Mariş,¹² R. Maruyama,⁴³ K. Mase,¹⁶ T. McElroy,²⁵ F. McNally,³⁶ K. Meagher,³⁸ A. Medina,²¹ M. Meier,¹⁶ S. Meighen-Berger,²⁷ J. Merz,¹ J. Micallef,²⁴ D. Mockler,¹² T. Montaruli,²⁸ R. W. Moore,²⁵ R. Morse,³⁸ M. Moulai,¹⁵ R. Naab,⁵⁹ R. Nagai,¹⁶ U. Naumann,⁵⁸ J. Necker,⁵⁹ L. V. Nguyen,²⁴ H. Niederhausen,²⁷ M. U. Nisa,²⁴ S. C. Nowicki,²⁴ D. R. Nygren,⁹ A. Obertacke Pollmann,⁵⁸ M. Oehler,³¹ A. Olivas,¹⁹ E. O'Sullivan,⁵⁷ H. Pandya,⁴² D. V. Pankova,⁵⁶ N. Park,³⁸ G. K. Parker,⁴ E. N. Paudel,⁴² L. Paul,⁴⁰ C. Pérez de los Heros,⁵⁷ S. Philippen,¹ D. Pieloth,²³ S. Pieper,⁵⁸ M. Pittermann,³² A. Pizzuto,³⁸ M. Plum,⁴⁰ Y. Popovych,³⁹ A. Porcelli,²⁹ M. Prado Rodriguez,³⁸ P. B. Price,⁸ B. Pries,²⁴ G. T. Przybylski,⁹ C. Raab,¹² A. Raissi,¹⁸ M. Rameez,²² K. Rawlins,³ I. C. Rea,²⁷ A. Rehman,⁴² R. Reimann,¹ G. Renzi,¹² E. Resconi,²⁷ S. Reusch,⁵⁹ W. Rhode,²³ M. Richman,⁴⁵ B. Riedel,³⁸ S. Robertson,^{8,9} G. Roellinghoff,⁵² M. Rongen,³⁹ C. Rott,^{49,52} T. Ruhe,²³ D. Ryckbosch,²⁹ D. Rysewyk Cantu,²⁴ I. Safa,^{14,38} J. Saffer,³² S. E. Sanchez Herrera,²⁴ A. Sandrock,²³ J. Sandroos,³⁹ M. Santander,⁵⁴ S. Sarkar,⁴⁴ S. Sarkar,²⁵ K. Satalecka,⁵⁹ M. Scharf,¹ M. Schaufel,¹ H. Schieler,³¹ P. Schlunder,²³ T. Schmidt,¹⁹ A. Schneider,³⁸ J. Schneider,²⁶ F. G. Schröder,^{31,42} L. Schumacher,²⁷ S. Sclafani,⁴⁵ D. Seckel,⁴² S. Seunarine,⁴⁷ A. Sharma,⁵⁷ S. Shefali,³² M. Silva,³⁸ B. Skrzypek,¹⁴ B. Smithers,⁴ R. Snihur,³⁸ J. Soedingrekso,²³ D. Soldin,⁴² C. Spannfellner,²⁷ G. M. Spiczak,⁴⁷ C. Spiering,^{59,†} J. Stachurska,⁵⁹ M. Stamatikos,²¹ T. Stanev,⁴² R. Stein,⁵⁹ J. Stettner,¹ A. Steuer,³⁹ T. Stezelberger,⁹ T. Stürwald,⁵⁸ T. Stuttard,²² G. W. Sullivan,¹⁹ I. Taboada,⁶ F. Tenholt,¹¹ S. Ter-Antonyan,⁷ S. Tilav,⁴² F. Tischbein,¹ K. Tollefson,²⁴ L. Tomankova,¹¹ C. Tönnis,⁵³ S. Toscano,¹² D. Tosi,³⁸ A. Trettin,⁵⁹ M. Tselengidou,²⁶ C. F. Tung,⁶ A. Turcati,²⁷ R. Turcotte,³¹ C. F. Turley,⁵⁶ J. P. Twagirayezu,²⁴ B. Ty,³⁸ M. A. Unland Elorrieta,⁴¹ N. Valtonen-Mattila,⁵⁷ J. Vandenbroucke,³⁸ N. van Eijndhoven,¹³ D. Vannerom,¹⁵ J. van Santen,⁵⁹ S. Verpoest,²⁹ M. Vraeghe,²⁹ C. Walck,⁵⁰ A. Wallace,² T.

B. Watson,⁴ C. Weaver,²⁴ P. Weigel,¹⁵ A. Weindl,³¹ M. J. Weiss,⁵⁶ J. Weldert,³⁹ C. Wendt,³⁸ J. Werthebach,²³ M. Weyrauch,³² B. J. Whelan,² N. Whitehorn,^{24,35} C. H. Wiebusch,¹ D. R. Williams,⁵⁴ M. Wolf,²⁷ K. Woschnagg,⁸ G. Wrede,²⁶ J. Wulff,¹¹ X. W. Xu,⁷ Y. Xu,⁵¹ J. P. Yanez,²⁵ S. Yoshida,¹⁶ S. Yu,²⁴ T. Yuan,³⁸ and Z. Zhang⁵¹

(IceCube Collaboration)

¹*III. Physikalisches Institut, RWTH Aachen University, D-52056 Aachen, Germany*

²*Department of Physics, University of Adelaide, Adelaide, 5005, Australia*

³*Dept. of Physics and Astronomy, University of Alaska Anchorage,
3211 Providence Dr., Anchorage, AK 99508, USA*

⁴*Dept. of Physics, University of Texas at Arlington,
502 Yates St., Science Hall Rm 108,
Box 19059, Arlington, TX 76019, USA*

⁵*CTSPS, Clark-Atlanta University, Atlanta, GA 30314, USA*

⁶*School of Physics and Center for Relativistic Astrophysics,
Georgia Institute of Technology, Atlanta, GA 30332, USA*

⁷*Dept. of Physics, Southern University, Baton Rouge, LA 70813, USA*

⁸*Dept. of Physics, University of California, Berkeley, CA 94720, USA*

⁹*Lawrence Berkeley National Laboratory, Berkeley, CA 94720, USA*

¹⁰*Institut für Physik, Humboldt-Universität zu Berlin, D-12489 Berlin, Germany*

¹¹*Fakultät für Physik & Astronomie,
Ruhr-Universität Bochum, D-44780 Bochum, Germany*

¹²*Université Libre de Bruxelles, Science Faculty CP230, B-1050 Brussels, Belgium*

¹³*Vrije Universiteit Brussel (VUB),
Dienst ELEM, B-1050 Brussels, Belgium*

¹⁴*Department of Physics and Laboratory for Particle Physics and Cosmology,
Harvard University, Cambridge, MA 02138, USA*

¹⁵*Dept. of Physics, Massachusetts Institute of Technology, Cambridge, MA 02139, USA*

¹⁶*Dept. of Physics and Institute for Global Prominent Research,
Chiba University, Chiba 263-8522, Japan*

¹⁷*Department of Physics, Loyola University Chicago, Chicago, IL 60660, USA*

¹⁸*Dept. of Physics and Astronomy, University of Canterbury,*

Private Bag 4800, Christchurch, New Zealand

¹⁹*Dept. of Physics, University of Maryland, College Park, MD 20742, USA*

²⁰*Dept. of Astronomy, Ohio State University, Columbus, OH 43210, USA*

²¹*Dept. of Physics and Center for Cosmology and Astro-Particle Physics,
Ohio State University, Columbus, OH 43210, USA*

²²*Niels Bohr Institute, University of Copenhagen, DK-2100 Copenhagen, Denmark*

²³*Dept. of Physics, TU Dortmund University, D-44221 Dortmund, Germany*

²⁴*Dept. of Physics and Astronomy,
Michigan State University, East Lansing, MI 48824, USA*

²⁵*Dept. of Physics, University of Alberta,
Edmonton, Alberta, Canada T6G 2E1*

²⁶*Erlangen Centre for Astroparticle Physics,
Friedrich-Alexander-Universität Erlangen-Nürnberg, D-91058 Erlangen, Germany*

²⁷*Physik-department, Technische Universität München, D-85748 Garching, Germany*

²⁸*Département de physique nucléaire et corpusculaire,
Université de Genève, CH-1211 Genève, Switzerland*

²⁹*Dept. of Physics and Astronomy,
University of Gent, B-9000 Gent, Belgium*

³⁰*Dept. of Physics and Astronomy,
University of California, Irvine, CA 92697, USA*

³¹*Karlsruhe Institute of Technology,
Institute for Astroparticle Physics, D-76021 Karlsruhe, Germany*

³²*Karlsruhe Institute of Technology,
Institute of Experimental Particle Physics, D-76021 Karlsruhe, Germany*

³³*Dept. of Physics and Astronomy,
University of Kansas, Lawrence, KS 66045, USA*

³⁴*SNOLAB, 1039 Regional Road 24,
Creighton Mine 9, Lively, ON, Canada P3Y 1N2*

³⁵*Department of Physics and Astronomy,
UCLA, Los Angeles, CA 90095, USA*

³⁶*Department of Physics, Mercer University, Macon, GA 31207-0001, USA*

³⁷*Dept. of Astronomy, University of Wisconsin-Madison, Madison, WI 53706, USA*

- ³⁸*Dept. of Physics and Wisconsin IceCube Particle Astrophysics Center,
University of Wisconsin–Madison, Madison, WI 53706, USA*
- ³⁹*Institute of Physics, University of Mainz,
Staudinger Weg 7, D-55099 Mainz, Germany*
- ⁴⁰*Department of Physics, Marquette University, Milwaukee, WI, 53201, USA*
- ⁴¹*Institut für Kernphysik, Westfälische
Wilhelms-Universität Münster, D-48149 Münster, Germany*
- ⁴²*Bartol Research Institute and Dept. of Physics and Astronomy,
University of Delaware, Newark, DE 19716, USA*
- ⁴³*Dept. of Physics, Yale University, New Haven, CT 06520, USA*
- ⁴⁴*Dept. of Physics, University of Oxford,
Parks Road, Oxford OX1 3PU, UK*
- ⁴⁵*Dept. of Physics, Drexel University,
3141 Chestnut Street, Philadelphia, PA 19104, USA*
- ⁴⁶*Physics Department, South Dakota School of
Mines and Technology, Rapid City, SD 57701, USA*
- ⁴⁷*Dept. of Physics, University of Wisconsin, River Falls, WI 54022, USA*
- ⁴⁸*Dept. of Physics and Astronomy,
University of Rochester, Rochester, NY 14627, USA*
- ⁴⁹*Department of Physics and Astronomy,
University of Utah, Salt Lake City, UT 84112, USA*
- ⁵⁰*Oskar Klein Centre and Dept. of Physics,
Stockholm University, SE-10691 Stockholm, Sweden*
- ⁵¹*Dept. of Physics and Astronomy,
Stony Brook University, Stony Brook, NY 11794-3800, USA*
- ⁵²*Dept. of Physics, Sungkyunkwan University, Suwon 16419, Korea*
- ⁵³*Institute of Basic Science, Sungkyunkwan University, Suwon 16419, Korea*
- ⁵⁴*Dept. of Physics and Astronomy,
University of Alabama, Tuscaloosa, AL 35487, USA*
- ⁵⁵*Dept. of Astronomy and Astrophysics,
Pennsylvania State University, University Park, PA 16802, USA*
- ⁵⁶*Dept. of Physics, Pennsylvania State University, University Park, PA 16802, USA*

⁵⁷*Dept. of Physics and Astronomy,*

Uppsala University, Box 516, S-75120 Uppsala, Sweden

⁵⁸*Dept. of Physics, University of Wuppertal, D-42119 Wuppertal, Germany*

⁵⁹*DESY, D-15738 Zeuthen, Germany*

(Dated: March 19, 2022)

Abstract

The advent of multi-messenger astronomy has allowed for new types of source searches by neutrino detectors. We present the results of the first search for 0.5 - 5 GeV astrophysical neutrinos emitted from all compact binary mergers, i.e., binary black hole, neutron star black, mass gap and binary neutron star mergers, detected by the LIGO and Virgo interferometers during their three first runs of observation. We use an innovative approach that lowers the energy threshold from ~ 10 GeV to ~ 0.5 GeV and searches for an excess of GeV-scale events during astrophysical transient events. No significant excess was found from the studied mergers, and there is currently no hint of a population of GeV neutrino emitters found in the IceCube data.

The first direct detection of gravitational waves by the LIGO interferometers [1] followed by three successful observing runs by the LIGO and Virgo collaborations (LVC) [2–4], have brought new opportunities in multi-messenger astronomy. While the first observed object was a binary black hole merger (BBH) [1], other compact binary merger types have since been reported: binary neutron star (BNS) mergers [5, 6], neutron star-black hole (NSBH) mergers [4, 7], and mergers involving compact objects with mass between the heaviest known neutron stars and the lightest known black holes (“Mass-gap”) [4, 7]. The astroparticle and astrophysics communities have carried out follow-up observations for every gravitational wave candidate reported by LIGO and Virgo [8–14]. Identifying a potential counterpart in electromagnetic waves and/or neutrinos can provide a multi-messenger picture of the studied object and can help constrain physical parameters of the sources, such as their surrounding density, understand acceleration mechanisms, and place constraints on fundamental physics, as has been done for the binary neutron star merger of August 17th, 2017 [5].

High-energy neutrino observatories have so far searched for neutrino counterparts in the TeV-PeV range, where astrophysical neutrinos emerge above the background of atmospheric neutrinos created by the interaction of cosmic rays with atmospheric nuclei [12, 14]. The GeV energy domain has not yet been extensively explored in terms of astrophysical neutrino observations. Only a few searches reported upper limits in the single and multi-GeV range [15–18] so far. Considering that astrophysical neutrino fluxes likely exhibit a power-

* also at Università di Padova, I-35131 Padova, Italy

† also at National Research Nuclear University, Moscow Engineering Physics Institute (MEPhI), Moscow 115409, Russia

‡ now at Université de Paris, CNRS, Astroparticule et Cosmologie, F-75013 Paris, France

§ also at Earthquake Research Institute, University of Tokyo, Bunkyo, Tokyo 113-0032, Japan

law decrease with energy, one can expect that neutrino telescopes sensitive to this energy range could allow us to probe larger neutrino fluxes and possibly identify new astrophysical neutrino sources. Until 2016, the Super-Kamiokande (SK) detector [19], optimized for neutrinos in the MeV - GeV range, was the only neutrino detector providing limits on the astrophysical neutrino flux in the GeV regime. It has set, among others, limits for the first detected gravitational wave events, GW150914 and GW151226, and GW170817, the binary neutron star merger [15, 16].

Part of the population detected by the LIGO and Virgo instruments may be associated with at least a fraction of the electromagnetically-detected gamma-ray bursts (GRBs) [20]. In such scenario, the neutrino production is expected to come from different processes depending on the considered energy range. While TeV neutrinos are predicted as a consequence of the internal shocks in the prompt emission phase of GRBs [21], GeV neutrinos could be produced by collisions of neutrons and protons following their decoupling during the acceleration phase [22]. Besides offering evidence of hadronic acceleration mechanisms, the detection of GeV neutrinos from GRBs would also constitute a probe of the target density surrounding the astrophysical object, allowing better constraints of the environments, acceleration processes, and progenitors of these phenomena [23–25].

In this paper, we report on a search for 0.5 - 5 GeV neutrinos, using the IceCube Neutrino Observatory (IceCube), from compact binary mergers detected by the LIGO and Virgo interferometers during the first three runs of observations [3, 4, 7]. Searching for GeV neutrinos with IceCube is challenging for several reasons. First, the atmospheric neutrino background dominates over most astrophysical sources at this energy. As we focus on transient events, we have used the timing coincidence with the gravitational wave detection to integrate the background only over short time windows. Secondly, no reconstruction of the incoming neutrino direction is feasible in IceCube at this energy, so we searched for an increase in the number of GeV events compared with the off-time region. We describe hereafter the use of IceCube for GeV neutrino detection as well as the searches that were carried out and their results. A discussion of the results, including a comparison of existing limits on the neutrino flux emitted from these objects is then presented. We conclude the paper with the prospects for similar searches in the coming decade.

USING THE ICECUBE NEUTRINO OBSERVATORY IN THE GEV ENERGY RANGE

The IceCube Neutrino Observatory is a cubic-kilometer neutrino detector installed in the ice at the geographic South Pole between depths of 1450 m and 2450 m [26]. It includes 5160 digital optical modules (DOMs) distributed along 86 strings deployed within the detector volume. This includes a lower energy infill detector, the DeepCore subarray, which includes 8 densely instrumented strings with smaller vertical spacing between its optical modules (7 m versus 17 m) and smaller horizontal spacing between its strings (72 m on average versus 125 m) [27]. When a neutrino interacts inside or in the surrounding medium of the detector, the subsequent electromagnetic and/or hadronic cascade produces Cherenkov photons that can be detected by one or more DOMs.

While IceCube was originally optimized to detect TeV neutrinos, the Collaboration has previously demonstrated the ability to extend the sensitivity to a wider energy range by the use of DeepCore, as it allows searches for neutrino interactions down to 5.6 GeV (see e.g., [28]). Besides a higher density of optical modules, a softer trigger condition has been implemented in DeepCore to improve its sensitivity to lower neutrino energies. A detailed description of the event selection developed in view of extracting GeV neutrino events from the IceCube data and its inherent systematic uncertainties is presented in [29]. A GeV neutrino interaction produces a cascade and, depending on the interaction channel, also a short track, emitting light close to the interaction vertex, resulting in a small number of causally connected DOMs. The rejection of high-energy i.e., > 5 GeV, events originating from atmospheric muons or neutrinos, produced by the interaction of cosmic rays with atmospheric nuclei, is done by placing strong upper constraints on the number of optical modules triggered by the interactions. The main obstacle is identifying GeV neutrino interactions in IceCube among a background due to random DOM noise, which also trigger the detector with a pattern similar to that expected from a low-energy neutrino.

A detailed simulation of DOM noise hits in the detector helps to estimate the potential contamination of accidental triggers, hereafter referred to as “noise events”. These include uncorrelated thermal noise, uncorrelated radioactive noise, and correlated scintillation noise [30–32]. About 6 Hz of noise events that were part of the initial 1400 Hz of data satisfies the constraints on the number of triggered optical modules and constitutes the

dominant contribution in the event sample. By requiring the distance between every pair of hits divided by the time separation between them to be consistent with the speed of light in ice, the selection ensures causality between pairs of hits. Applying this causality condition reduces the rate of detector noise events from 6 Hz to 0.2 Hz. Additional variables sensitive to the morphology of the events help to create a cleaner GeV neutrino sample. Among these, cuts on the estimated depth of the interaction point and the charge located around it as well as the total charge of the event reduce the data rate down to 0.02 Hz, as described in [29]. More than 40% of the neutrino interactions between 0.5 GeV and 5 GeV generated with GENIE 2.8.6 [33] following a generic E^{-2} spectrum pass this selection with respect to those passing the online trigger and are considered in the analysis as GeV event candidates. The final rate, being dominated by remaining noise events, is larger than the expectation of atmospheric neutrinos, estimated to occur at the mHz level. The all-interaction-channel effective areas for electron and muon neutrinos passing the described selection is shown in Fig. 1.

DESCRIPTIONS AND RESULTS OF THE SEARCHES

For each binary merger reported by LIGO and Virgo in GWTC-1 [3], GWTC-2 [4], or in GraceDB for O3b [7], we have counted the number of low-energy neutrino candidate events passing the selection previously described. These numbers are to be compared to background estimates based on 2659 background-only time windows of 1000 s when no GRBs were reported based on GRBweb¹, an all-inclusive catalog of gamma-ray bursts. This on-time/off-time strategy has been used to estimate the significance of the GeV neutrino observation for each binary merger. To ensure good quality of the sample used to search for a GeV neutrino counterpart of compact binary mergers, several checks were performed prior to the unblinding of the data. In addition to the automated data quality checks performed on IceCube data to monitor the detector stability continuously [26], we checked the background rate in an 8h-time window preceding the astrophysical merger to evaluate if the 0.02 Hz background-only data rate and its statistical fluctuations are identical to that of archival data. We also checked that the GeV neutrino candidate events detected during the time windows of the searches were distributed across the detector to exclude

¹ https://user-web.icecube.wisc.edu/~grbweb_public/

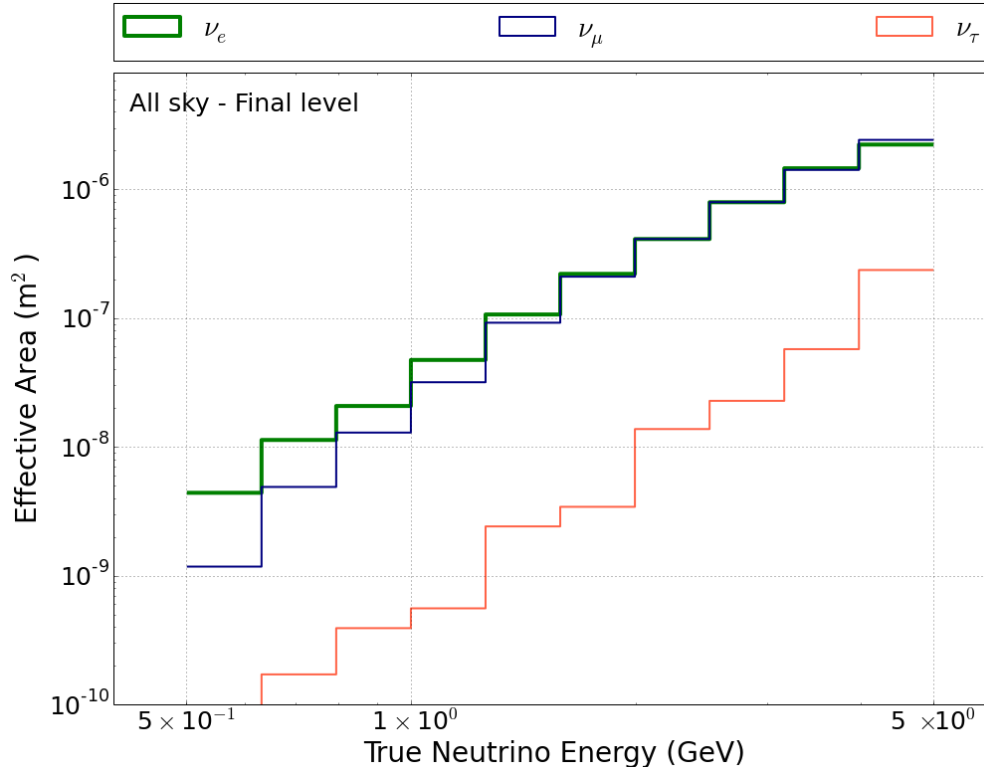


FIG. 1: Effective areas including all possible interaction channels for each flavor (neutrino and anti-neutrino). Charged current interactions for tau neutrinos only become relevant at the upper limit of this energy range due to the mass of the tau lepton. At low energies, electron neutrinos have a larger effective area than muon neutrinos as the produced lepton in charged current interactions has a smaller mass and hence carries out more kinetic energy.

any potential detector effects causing several events to happen at a specific location. In order to further ensure data quality, a visual inspection of the events in the time window of interest was performed to validate the unblinded sample. The data recorded during each of the 72 gravitational wave candidates reported by LIGO and Virgo during their three runs of observations pass our data quality checks, with the exception of GW190513_205428 and GW190731_140936, for which the data taking in IceCube was not stable enough to provide a satisfactory GeV neutrino candidate sample.

We carried out two different GeV neutrino searches using the obtained data sample: a search for a prompt signal and a search in an extended time window.

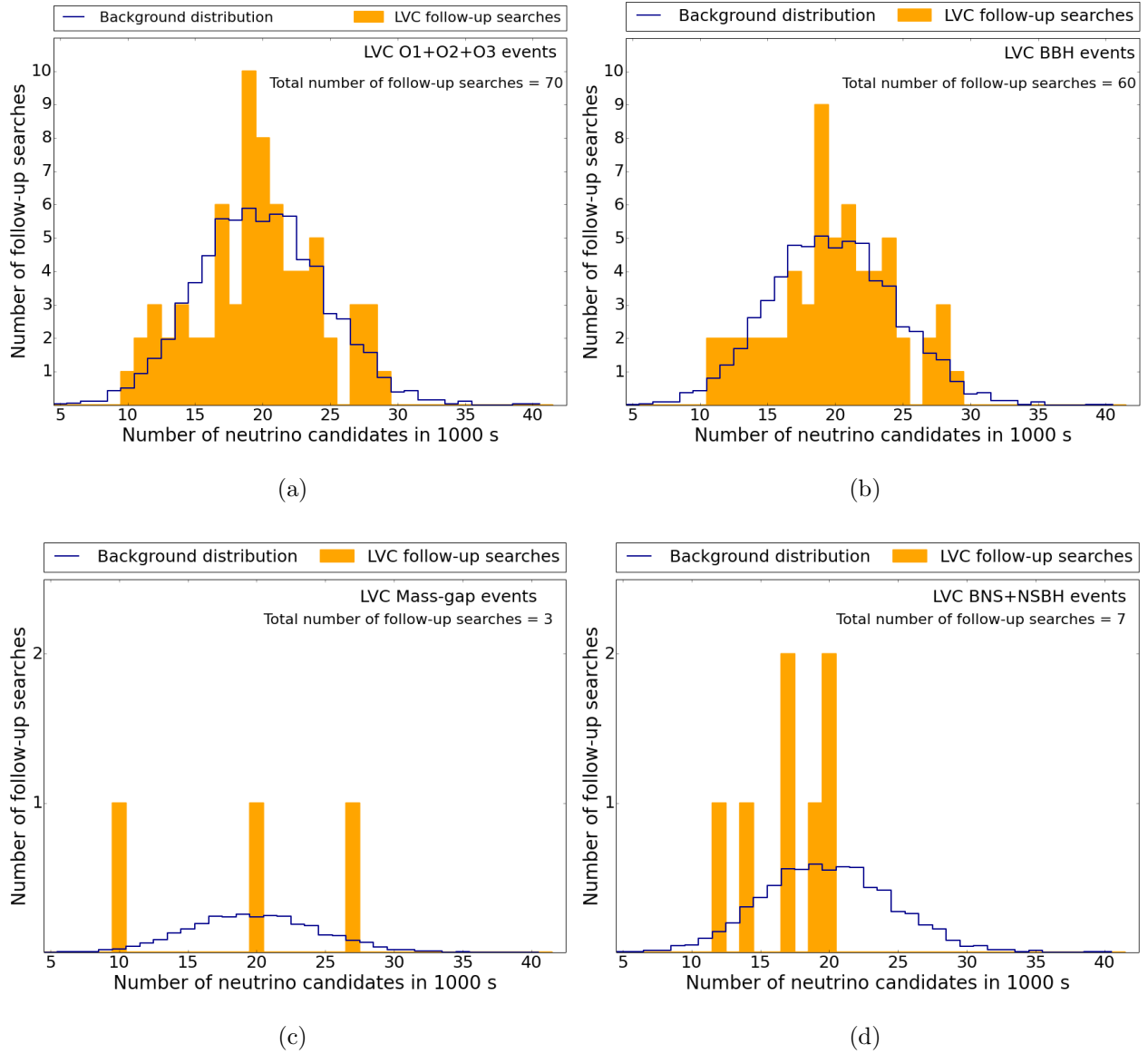


FIG. 2: The panel in Fig. 2a shows the background distribution (blue) and distribution of the number of low-energy candidate events detected during the 1000 s time window around compact binary mergers (orange). The other sub-figures show the distribution of the studied mergers as function of their progenitor types, namely BBH in Fig. 2b, Mass-gap candidates in Fig. 2c, and NSBH and BNS in Fig. 2d.

Search for a signal in an extended time window

Using the conservative time window derived in [34] based on precursor and afterglow electromagnetic data of GRBs, we have searched for an excess in the integrated number of

events in the $[t - 500\text{s}, t + 500\text{s}]$ around the merger time t reported by LVC. The number of candidate events associated with each compact binary merger candidate is reported in Table I. Figure 2 shows the distribution of 2659 time windows of 1000 s, obtained using IceCube data when no GRB was reported. In the same figure, the orange lines show the number of events passing our selection for each of the studied mergers. The sub-figures show the distribution of the studied mergers as functions of their progenitor types. The merger associated with the largest number of GeV neutrino candidate events is the BBH GW170608 with a total of 29 GeV-neutrino-like events recorded in IceCube during the 1000 s around the merger time. This merger lies in the 5 % tail of the background-only distribution. We can derive a 90% C.L. upper limit per merger candidate on the time-integrated all-flavor neutrino flux detected at Earth of $3.9 \times 10^4 \text{ cm}^{-2}$ assuming power-law emission with a spectral index of -2 between 0.5 GeV and 5 GeV.

Search for a prompt signal

In addition, we have carried out a search for a prompt signal for the LVC events that may be associated with the progenitors of short gamma-ray bursts. We focused on the BNS, NSBH, and Mass-gap events. Based on the first BNS detected, GW170817, and the subsequent GRB detected 1.7 s later by Fermi-GBM and Swift [5], we define $[t, t + 3 \text{ s}]$ as a time window for the search of a prompt signal, where t is the merger time reported by LVC [3, 4, 7]. For each of the analyzed mergers, no events were found in the three seconds following the merger time. We set a 90% C.L. upper limit per merger candidate of 1.2×10^4 neutrinos cm^{-2} on the time-integrated all-flavor neutrino flux over 3 s emitted by each of the progenitors between 0.5 GeV and 5 GeV.

Constraining the Presence of a Source Population

Using the results of the searches in an extended time window around the merger time, we have carried out a search for the presence of a source population. If a fraction of the studied mergers were GeV neutrino emitters, the detected neutrinos would add to the background, leading to an excess of mergers with a high number of corresponding neutrino candidate events in the 1000 s of interest. We have performed a Kolmogorov-Smirnov test to compare

the event distribution of mergers shown in orange in Fig. 2 and the background-only distribution (in blue in the same figure). Based on pseudo-experiment realizations of background distributions with the same number of follow-up searches, a p-value of 0.3 was obtained for the actual follow-up search distribution and therefore no source population was detected in the data.

Derivation of the isotropic-equivalent energy E_{iso} upper limit for the 3 s search for GW170817

A convenient way to compare the obtained limit with other constraints derived for similar compact binary mergers is to convert it into a limit on the isotropic-equivalent energy E_{iso} . This variable represents the energy flux at Earth multiplied by 4π times the square of the distance between the Earth and the source. Figure 3 shows a comparison of the all-flavor limit obtained on E_{iso} for GW170817 with similar constraints obtained by Super-Kamiokande in the 1.6 to 10^8 GeV energy range, when focusing on upward-going muons, and 100 MeV to 10 GeV for the all-flavor search [19]; the ANTARES [12] and IceCube [14] limits in the $\sim 10^2$ to $\sim 10^{11}$ GeV energy range are also displayed. All analyses have assumed neutrino production at the source following a power law with a spectral index of -2. While the limit obtained with the analysis presented in this paper is less stringent than some of the other constraints, it probes a lower energy range and thus different production mechanisms, as previously described. We note that the E_{iso} measured by the gamma-ray detection made by Fermi-GBM stands 5 orders of magnitude below the best constraints set on the time-integrated neutrino energy [12, 14], as shown in Fig. 3b.

CONCLUSION AND DISCUSSION

We have presented the first search for a 0.5 - 5 GeV neutrino counterpart to compact binary mergers using the IceCube Neutrino Observatory. The main results are:

- The search in an extended time window around the compact binary merger time $[t - 500 \text{ s}, t + 500 \text{ s}]$ led to no significant neutrino excess;
- For BNS, NSBH, and Mass-gap events, a neutrino search for prompt emission was carried out in the $[t, t + 3\text{s}]$ time window and no significant excess was found;

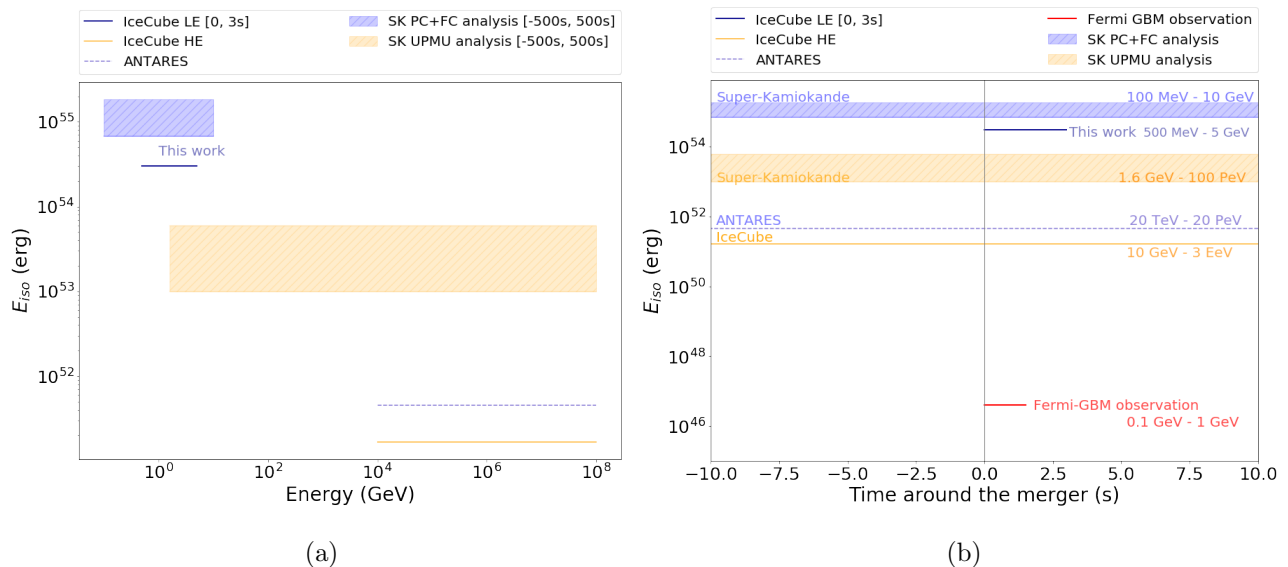


FIG. 3: Comparison of E_{iso} constraints as a function of the neutrino energy (left) and time around the merger (right, focusing on [-10 s, 10 s] around the merger), for GW170817. We compare the constraints set by the neutrino search presented in this work (IceCube LE, blue line) with the searches performed for the BNS GW170817 by Super-Kamiokande [16] (blue shaded (all-flavor) and orange shaded (muon neutrino) areas) and using high-energy neutrinos (ANTARES [12] (dashed blue line, all-flavor) and IceCube HE [14] (orange, muon neutrinos)). A time window of 3 s was used here, while 1000 s were integrated to obtain the constraints using high-energy neutrinos and Super-Kamiokande data. While Super-Kamiokande could in principle detect neutrinos in the PeV energy range, its effective area is significantly lower at these energies than that of large neutrino telescopes.

- Upper limits on the 0.5 - 5 GeV neutrino flux per binary compact merger were determined to be 1.2×10^4 and 3.9×10^4 neutrinos cm^{-2} for the 3 s and the 1000 s time windows, respectively;
- Our all-flavor upper limit on E_{iso} for the BNS of August 17th, 2017 improves the constraints in the GeV energy range for all-flavor neutrino searches compared to existing limits set by Super-Kamiokande and represents complementary information to high-energy neutrino searches from ANTARES and IceCube, and gamma-ray observations made by Fermi-GBM;
- No source population is detected when performing a shape analysis of the merger vs.

background-only event distributions, considering the number of neutrino candidate events per burst integrated over 1000 s time window.

This work validates the innovative approach required to allow IceCube to be sensitive in the 0.5 - 5 GeV energy range and confirms the feasibility to perform follow-up searches in this energy range. This approach will be used to carry out searches for neutrino counterparts of relevant astrophysical phenomena detected via gravitational or electromagnetic waves.

The main limitation of this search comes from the minimal trigger requirement in IceCube, i.e., 3 DOMs with coincident pulses within $2.5 \mu\text{s}$, which prevents some GeV neutrino interactions from being recorded. A separate data stream in IceCube, called HitSpooling [26], saves every single hit occurring in the detector, independent of the implemented trigger conditions. Sub-threshold neutrino interactions, lost in regular IceCube data, can be saved and studied. Using such a data stream would directly result in an increase of the sensitivity in the energy range studied in this paper. HitSpool data have significantly larger size than regular IceCube data, and cannot therefore be continuously saved. To take advantage of this additional data stream and the increased sensitivity it offers, we have created an alert system that saves HitSpool data based on the initial GCN circulars sent by the LIGO and Virgo collaborations. The system has successfully saved data for the alerts sent during their third run of observation and the data analysis is currently ongoing.

The current construction of KM3NeT/ORCA in the Mediterranean Sea [35, 36], and the deployment of the IceCube Upgrade [37] within IceCube, may improve the current detection capabilities between 0.5 and 5 GeV. These detectors will be equipped with multi-anode sensors allowing event directional reconstruction and better noise rejection. This will lead to a lower detection threshold and improved sensitivity. The increasing sensitivity of the gravitational wave interferometers will lead to a larger population to probe using GeV neutrino interactions, improving global constraints on the physics of gravitational wave sources.

ACKNOWLEDGMENTS

The IceCube collaboration acknowledges the significant contributions to this manuscript from Gwenhaël de Wasseige. We gratefully acknowledge the support from the following agencies and institutes: USA – U.S. National Science Foundation-Office of Polar Programs, U.S.

National Science Foundation-Physics Division, U.S. National Science Foundation-EPSCoR, Wisconsin Alumni Research Foundation, Center for High Throughput Computing (CHTC) at the University of Wisconsin–Madison, Open Science Grid (OSG), Extreme Science and Engineering Discovery Environment (XSEDE), Frontera computing project at the Texas Advanced Computing Center, U.S. Department of Energy-National Energy Research Scientific Computing Center, Particle astrophysics research computing center at the University of Maryland, Institute for Cyber-Enabled Research at Michigan State University, and Astroparticle physics computational facility at Marquette University; Belgium – Funds for Scientific Research (FRS-FNRS and FWO), FWO Odysseus and Big Science programmes, and Belgian Federal Science Policy Office (Belspo); Germany – Bundesministerium für Bildung und Forschung (BMBF), Deutsche Forschungsgemeinschaft (DFG), Helmholtz Alliance for Astroparticle Physics (HAP), Initiative and Networking Fund of the Helmholtz Association, Deutsches Elektronen Synchrotron (DESY), and High Performance Computing cluster of the RWTH Aachen; Sweden – Swedish Research Council, Swedish Polar Research Secretariat, Swedish National Infrastructure for Computing (SNIC), and Knut and Alice Wallenberg Foundation; Australia – Australian Research Council; Canada – Natural Sciences and Engineering Research Council of Canada, Calcul Québec, Compute Ontario, Canada Foundation for Innovation, WestGrid, and Compute Canada; Denmark – Villum Fonden and Carlsberg Foundation; New Zealand – Marsden Fund; Japan – Japan Society for Promotion of Science (JSPS) and Institute for Global Prominent Research (IGPR) of Chiba University; Korea – National Research Foundation of Korea (NRF); Switzerland – Swiss National Science Foundation (SNSF); United Kingdom – Department of Physics, University of Oxford. G. de Wasseige acknowledges support from the European Union’s Horizon 2020 research and innovation programme under the Marie Skłodowska-Curie grant agreement No 844138.

-
- [1] **LIGO** Scientific Collaboration and **Virgo** Collaboration, B. P. Abbott *et al.*, Phys. Rev. Lett. **116**, 061102 (2016).
 - [2] **LIGO** Scientific Collaboration, J. Aasi *et al.*, Class. Quantum Grav., **32**, 074001 (2015).
 - [3] **LIGO** Scientific Collaboration and **Virgo** Collaboration, B. P. Abbott *et al.*, GWTC-1, Phys. Rev. X, **9**, 031040 (2019).

- [4] **LIGO** Scientific Collaboration and **Virgo** Collaboration, B. P. Abbott *et al.*, GWTC-2, Report Number P2000061, arXiv:2010.14527.
- [5] **LIGO** Scientific Collaboration and **Virgo** Collaboration, Phys. Rev. Lett. **119**, 161101 (2017).
- [6] **LIGO** Scientific Collaboration and **Virgo** Collaboration, B. P. Abbott *et al.*, Astrophys. J. Lett. **892**, L3 (2020).
- [7] <https://gracedb.ligo.org/superevents/public/03/>, October 2020.
- [8] **LIGO** Scientific Collaboration and **Virgo** Collaboration, B. P. Abbott *et al.*, Astrophys. J. **875**, 2 (2019).
- [9] **IceCube** Collaboration, **LIGO** Scientific Collaboration and **Virgo** Collaboration, M. G. Aartsen *et al.*, Phys. Rev. D **90**, 102002 (2014).
- [10] **ANTARES** Collaboration, **IceCube** Collaboration, **LIGO** Scientific Collaboration and **Virgo** Collaboration, S. Adriàn-Martinez *et al.*, Phys. Rev. D **93**, 122010 (2016).
- [11] **ANTARES** Collaboration, **IceCube** Collaboration, **LIGO** Scientific Collaboration and **Virgo** Collaboration, A. Albert *et al.*, Phys. Rev. D **96**, 022005 (2017).
- [12] **ANTARES** Collaboration, **IceCube** Collaboration, **Pierre Auger** Collaboration, **LIGO** Scientific Collaboration and **Virgo** Collaboration, A. Albert *et al.*, Astrophys. J. **850**, 2 (2017).
- [13] **ANTARES** Collaboration, **IceCube** Collaboration, **LIGO** Scientific Collaboration and **Virgo** Collaboration, A. Albert *et al.*, Astrophys. J. **870**, 134 (2019).
- [14] **IceCube** Collaboration, M. G. Aartsen *et al.*, Astrophys. J. Lett. **898**, L10 (2020).
- [15] **Super-Kamiokande** Collaboration, K. Abe *et al.*, Astrophys. J. Lett. **830**, L11 (2016).
- [16] **Super-Kamiokande** Collaboration, K. Abe *et al.*, Astrophys. J. Lett. **857**, L4 (2018).
- [17] **IceCube** Collaboration, M. G. Aartsen *et al.*, Astrophys. J. **816**, 75 (2016).
- [18] **IceCube** Collaboration, R. Abbasi *et al.*, arXiv:2011.05096.
- [19] S. Fukuda *et al.*, Nucl. Instrum. Meth. **501**, 2 (2003).
- [20] K. Murase and I. Bartos, Ann. Rev. Nucl. Part. Sci. **69**, 477 (2019).
- [21] F. Halzen, D. Hooper, Rept. Prog. Phys. **65**, 1025 (2002).
- [22] K. Asano, K. Murase, Adv. Astron., 568516 (2015).
- [23] S. Kimura *et al.*, Phys. Rev. D **98**, 043020 (2018).
- [24] S. Razzaque, P. Meszaros, and E. Waxman, Phys. Rev. D **68**, 083001 (2003).
- [25] I. Bartos, B. Dasgupta, and S. Marka, Phys. Rev. D **86**, 083007 (2012).

- [26] **IceCube** Collaboration, M. G. Aartsen *et al.*, JINST **12**, P03012 (2017).
- [27] **IceCube** Collaboration, R. Abbasi *et al.*, Astropart. Phys. **35**, 615 (2012).
- [28] **IceCube** Collaboration, M. G. Aartsen *et al.*, Phys. Rev. D **99**, 3 (2019).
- [29] **IceCube** Collaboration, R. Abbasi *et al.*, Phys. Rev. D **103**, 102001 (2021).
- [30] **IceCube** Collaboration, R. Abbasi *et al.*, Nucl. Instrum. Meth. A **618**, 139 (2010).
- [31] **IceCube** Collaboration, R. Abbasi *et al.*, Nucl. Instrum. Meth. A **601**, 294 (2009).
- [32] M. Larson, M.S. thesis, University of Alabama, Tuscaloosa (2013).
- [33] C. Andreopoulos *et al.*, Nucl. Instrum. Meth. A **614**, 87 (2010).
- [34] B. Baret *et al.*, Astropart. Phys. **35**, 1 (2011).
- [35] **KM3NeT** Collaboration, S. Adrià-Martinez *et al.*, Journal of Physics G: Nuclear and Particle Physics, **43**, 8 (2016).
- [36] G. de Wasseige for the **KM3NeT** Collaboration, PoS(ICRC2019) 934.
- [37] A. Ishihara for the **IceCube** Collaboration, PoS(ICRC2019)1031.

TABLE I: List of compact binary mergers that are considered in this work. We quote the type announced by LVC in GWTC-1 and GWTC-2 [3, 4] or the most probable astrophysical type of the merger as reported by LVC in GraceDB for O3b [7], and the number of low-energy neutrino events passing our selection during the considered 1000 s time window. The estimated background is 0.020 ± 0.002 Hz.

Name	Time	Reported type	Number of events
O1			
GW150914	Sept. 14, 2015 - 09:50:45 UTC	BBH	23
GW151012	Oct. 10, 2015 - 09:54:43 UTC	BBH	22
GW151226	Dec. 26, 2015 - 03:38:53 UTC	BBH	25
O2			
GW170104	Jan. 04, 2017 - 10:11:58 UTC	BBH	23
GW170608	June 08, 2017 - 02:01:16 UTC	BBH	29
GW170729	July 07, 2017 - 18:56:29 UTC	BBH	19
GW170809	Aug. 09, 2017 - 08:28:21 UTC	BBH	19
GW170814	Aug 14, 2017 - 10:30:43 UTC	BBH	19
GW170817	Aug. 17, 2017 - 12:41:04 UTC	BNS	12
GW170818	Aug. 18, 2017 - 02:25:09 UTC	BBH	24
GW170823	Aug. 23, 2017 - 13:13:58 UTC	BBH	22
O3a			
GW190408_181802	April 8, 2019, 18:18:02 UTC	BBH	13
GW190412	April 12, 2019, 05:30:44 UTC	BBH	20
GW190413_052954	April 13, 2019, 05:29:54 UTC	BBH	17
GW190413_134308	April 13, 2019, 13:43:08 UTC	BBH	21
GW190421_213856	April 21, 2019, 21:38:56 UTC	BBH	14
GW190424_180648	April 24, 2019, 18:06:48 UTC	BBH	17
GW190425	April 25, 2019, 08:18:05 UTC	BNS	20
GW190426_152155	April 26, 2019, 15:21:55 UTC	NSBH	17
GW190503_185404	May 3, 2019, 18:54:04 UTC	BBH	22
GW190512_180714	May 12, 2019, 18:07:14 UTC	BBH	19
GW190513_205428	May 13, 2019, 20:54:28 UTC	BBH	–

Name	Time	Reported type (probability)	Number of events
O3a			
GW190514.065416	May 14, 2019, 06:54:16 UTC	BBH	17
GW190517.055101	May 17, 2019, 05:51:01 UTC	BBH	24
GW190519.153544	May 19, 2019, 15:35:44 UTC	BBH	12
GW190521	May 21, 2019, 03:02:29 UTC	BBH	27
GW190521.074359	May 21, 2019, 07:43:59 UTC	BBH	20
GW190527.092055	May 27, 2019, 09:20:55 UTC	BBH	13
GW190602.175927	June 2, 2019, 17:59:27 UTC	BBH	15
GW190620.030421	June 20, 2019, 03:04:21 UTC	BBH	25
GW190630.185205	June 30, 2019, 18:52:05 UTC	BBH	19
GW190701.203306	July 1, 2019, 20:33:06 UTC	BBH	28
GW190706.222641	July 6, 2019, 22:26:41 UTC	BBH	21
GW190707.093326	July 7, 2019, 09:33:26 UTC	BBH	21
GW190708.232457	July 8, 2019, 23:24:57 UTC	BBH	19
GW190719.215514	July 19, 2019, 21:55:14 UTC	BBH	18
GW190720.000836	July 20, 2019, 00:08:36 UTC	BBH	17
GW190727.060333	July 27, 2019, 06:03:33 UTC	BBH	19
GW190728.064510	July 28, 2019, 06:45:10 UTC	BBH	27
GW190731.140936	July 31, 2019, 14:09:36 UTC	BBH	–
GW190803.022701	August 3, 2019, 02:27:01 UTC	BBH	22
GW190814	Aug. 14, 2019, 21:10:39 UTC	BBH	21
GW190828.063405	Aug. 28, 2019, 06:34:05 UTC	BBH	11
GW190828.065509	Aug. 28, 2019, 06:55:09 UT	BBH	14
GW190909.114149	Sept. 9, 2019, 11:41:49 UTC	BBH	17
GW190910.112807	Sept. 10, 2019, 11:28:07 UTC	BBH	15
GW190915.235702	Sept. 15, 2019 - 23:57:02 UTC	BBH	23
GW190924.021846	Sept. 24, 2019 - 02:18:46 UTC	BBH	24
GW190929.012149	Sept. 29, 2019, 01:21:49 UTC	BBH	16
GW190930.133541	Sept. 30, 2019 - 13:35:41 UTC	Mass-gap	10

Name	Time	Reported type (probability)	Number of events
O3b			
S191105e	Nov. 5, 2019 - 14:35:21 UTC	BBH (95%)	19
S191109d	Nov. 9, 2019 - 01:07:17 UTC	BBH (>99%)	11
S191129u	Nov. 29, 2019 - 13:40:29 UTC	BBH (>99%)	18
S191204r	Dec. 4, 2019 - 17:15:26 UTC	BBH (>99%)	24
S191205ah	Dec. 5, 2019 - 21:52:08 UTC	NSBH (93%)	14
S191213g	Dec. 13, 2019 - 04:34:08 UTC	BNS (77%)	19
S191215w	Dec. 15, 2019 - 22:30:52 UTC	BBH (>99%)	21
S191216ap	Dec. 16, 2019 - 21:33:38 UTC	BBH (99%)	12
S191222n	Dec. 22, 2019 - 03:35:37 UTC	BBH (>99%)	16
S200105ae	Jan. 5, 2020 - 16:24:26 UTC	NSBH (3%)	17
S200112r	Jan. 12, 2020 - 15:58:38 UTC	BBH (>99%)	20
S200115j	Jan. 15, 2020 - 04:23:09 UTC	Mass-gap (>99%)	27
S200128d	Jan. 28, 2020 - 02:20:11 UTC	BBH (97%)	24
S200129m	Jan. 29, 2020 - 06:54:58 UTC	BBH (>99%)	28
S200208q	Feb. 8, 2020 - 13:01:17 UTC	BBH (99%)	20
S200213t	Feb. 13, 2020 - 04:10:40 UTC	BNS (63%)	20
S200219ac	Feb. 19, 2020 - 09:44:15 UTC	BBH (96%)	28
S200224ca	Feb. 24, 2020 - 22:22:34 UTC	BBH (>99%)	23
S200225q	Feb. 25, 2020 - 06:04:21 UTC	BBH (96%)	18
S200302c	March 2, 2020 - 01:58:11 UTC	BBH (89%)	19
S200311g	March 11, 2020 - 11:58:53 UTC	BBH (>99%)	21
S200316bj	March 16, 2020 - 21:57:56 UTC	Mass-gap (>99%)	20